Synchronized Laser Modules With Frequency Offset up to 50 GHz for Ultra-Accurate Long-Distance Fiber Optic Time Transfer Links

Łukasz Śliwczyński, *Member, IEEE*, Przemyslaw Krehlik, Łukasz Buczek, and Harald Schnatz

***Abstract*—The paper is focused on a systematic investigation of the circuits for active stabilization of the frequency offset between two semiconductorn ultra-accurate fiber optic time transfer systems. The frequency offset is increased up to 50 GHz, which can be achieved not only with relatively low-noise integrated tunable laser assemblies, but also with ordinary, telecom-grade, distributed feedback lasers. The paper starts by determining the general frequency accuracy and stability, required to keep the uncertainty contribution of the stabilization circuit at a negligible level (assumed here as 1 ps) compared to other contributions of the overall uncertainty of the link calibration. Next, the technical details of the essential building block of the system discussed, which is required to convert the high-frequency offset to lower frequencies to allow convenient frequency measurement, are analyzed. Experimental circuits built with commercially available millimeter wave integrated circuits were tested with the frequency offset complying with telecom dense wavelength division multiplex standards, equal to 12.5 GHz, 25 GHz and 50 GHz. It was found that such stabilization circuits can cause substantial systematic errors, which are related to lasers' phase noise and the operation with low input optical powers (below −39 dBm in evaluated circuits). These effects were investigated experimentally in detail and countermeasures were proposed.**

***Index Terms*—Calibration uncertainty, fiber optic, laser wavelength stabilization, systematic frequency error, time transfer.**

I. Introduction

TIME and frequency are the quantities that can be currently measured and generated with the highest possible accuracies. Thanks to the continuous progress in the field of atomic clocks, which has been started in 1955 with the first cesium clock developed by Essen and Parry at NPL, showing accuracy of 10^{-10} [1]. Nowadays, a great number of commercial Cs-clocks is employed around the world, with accuracies around a few times 10^{-13}, as well as Cs-fountains, showing accuracies about three orders of magnitude better [2], [3] and operated by time and frequency (T&F) laboratories in many National Metrology Institutions (NMI). Recent progress in the field of optical clocks has pushed the relative accuracy towards 10^{-18} [4], [5] and has started an ongoing discussion about possible redefinition of the SI unit of time – the second within an envisaged future [5].

Apart from being an autonomous research discipline, accurate and stable T&F sources (i.e., clocks) are required in many areas of human activities, ranging from scientific applications, like fundamental physics [6], through spectroscopy [7], radio-astronomy [8]–[10], relativistic geodesy [11] and ending with more practical applications, like generation of timescales, positioning and navigation [12], synchronization or supervision of telecommunication networks [13], [14], power grids control [15], or even applications in the financial sector [16].

The development of accurate T&F sources and their applications would not be possible without the technical means to send their signals over long distances. This is necessary, on the one hand, for the provision of their signals outside specialized T&F laboratories and, on the other hand, for the monitoring of the clocks (which requires continuous comparison with other accurate clocks). Traditional methods, exploiting global navigation satellite system (GNSS) [17], like GPS, Galileo, Glonass or BeiDou, or using geostationary satellites [18], are often insufficient in terms of either accuracy, the time required to perform comparison, the vulnerability of satellite signals to external interference, or too strong dependency of critical infrastructure on GNSS (see, e.g., [19]). This resulted in the development of new methods of T&F transfer that exploit an optical fiber as a transmission medium [20]–[25].

Typical fiber optic T&F transfer link uses two counter-propagating optical signals, intensity modulated with a digital waveform carrying frequency and one pulse per second (PPS) time markers, which are sent over the same fiber. The use of the same fiber is essential to compensate for the fiber noise resulting from changing environmental conditions, like temperature, mechanical stress or vibrations that all affect the propagation delay of transmitted signals. As changes of the propagation conditions in both directions of the same fiber are closely coupled, it can be shown that they cancel out significantly in case of bidirectional signaling that has been proved in numerous experiments [20]–[27]. Such approach can work either in a two-way [20]–[22] or

Manuscript received November 9, 2021; revised January 4, 2022; accepted January 25, 2022. Date of publication February 1, 2022; date of current version May 2, 2022. This work was supported by the Polish National Science Center under Grant 2017/26/M/ST7/00128. *(Corresponding author: Łukasz Śliwczyński.)*

Łukasz Śliwczyński, Przemyslaw Krehlik, and Łukasz Buczek are with the Department of Computer Science, Electronics, and Telecommunications, AGH University of Science and Technology, 30-059 Krakow, Poland (e-mail: sliwczyn@agh.edu.pl; krehlik@agh.edu.pl; lbuczek@agh.edu.pl).

Harald Schnatz is with Quantum Optics and the Unit of Length, Physikalisch-Technische Bundesanstalt (PTB), 38116 Braunschweig, Germany (e-mail: harald.schnatz@ptb.de).

Color versions of one or more figures in this article are available at https://doi.org/10.1109/JLT.2022.3147591.

Digital Object Identifier 10.1109/JLT.2022.3147591

in a feedback [23]–[27] configuration, the last one allowing not only to reduce the fiber noise, but also to stabilize the propagation delay of the link. This feature is important for T&F distribution, where a distant user requires an access to accurate and stable signals without necessity of operating its own clock. Stabilized links allow also accurate time distribution where the link delay causing the offset to the timescale realization is not only stable but also either known, or even aligned to zero [28].

For ultimate transfer accuracy with a long-term uncertainty in the order of a few picoseconds and links spanning hundredths of kilometers, the frequency accuracy and stability of the laser sources used to generate the optical signals propagating along the fiber (these are typically semiconductor telecom-grade distributed feedback lasers - DFB) is a crucial parameter [13], [23]–[27]. The fiber's chromatic dispersion causes a propagation delay asymmetry when the frequencies of the two counter-propagating lasers differ. This asymmetry can be determined and accounted for through the link calibration, but the accuracy of time transfer depends critically on the accuracy and stability of laser's frequency difference.

The problem of lasers frequency accuracy can be solved using some kind of external wavelength standard. Often a compact version of a Fabry-Perot etalon is exploited, called a wavelength locker. This is a standard solution used in many dense wavelength division multiplexed (DWDM) systems, and is widely available (see, e.g., [29]). Such an approach, however, limits the long-term wavelength accuracy to around 1 GHz (i.e., to about 8 pm), which is perfectly enough for the telecom requirements, but is insufficient for picoseconds-accurate time transfer. Using better wavelength references, like e.g., a gas absorption cell or more sophisticated optical cavities is possible, but only at the expense of increased complexity, size and cost [30].

Another possibility, which was suggested for the first time in [27], and is now thoroughly analyzed in this paper, is to stabilize the beat note between the involved lasers, which is equivalent to keeping their frequency offset constant. Thus, instead of relying on the accuracy of two independent optical etalons, the entire wavelength stabilization system can be realized in the electrical domain.

A system of the abovementioned type can be built relatively easily, using either frequency or even phase locking, when the frequency offset between the two lasers is in the order of a few GHz. Such small offsets are, however, useful only in case of short links, not exceeding some 40 to 50 kilometers [23], unless sophisticated laser switching techniques are involved [26]. This is because of Rayleigh backscattering, which causes a substantial level of intensity noise [31]. To mitigate this problem optical filters are necessary, which are in practice available at reasonable cost only for the frequencies defined by the International Telecommunications Union (ITU) in Recommendation G.694.1 for DWDM networks. Desirable offsets are thus multiples of the minimum channel spacing, and are equal to 12.5 GHz, 25 GHz, 50 GHz or 100 GHz. With the advent of modern millimeter wave integrated circuits, like low-noise amplifiers (LNA), mixers, frequency phase locked loop (PLL) synthesizers and high speed frequency dividers, the offset frequencies up to 50 GHz are possible.

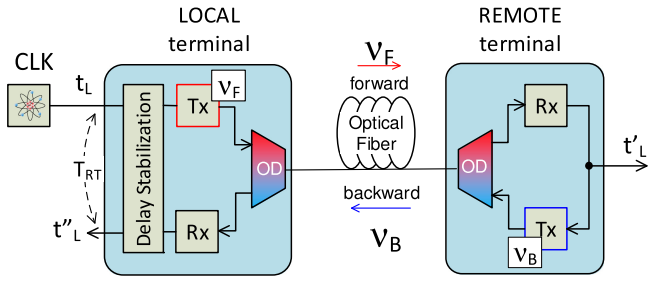

Fig. 1. Generic block diagram of the time transfer link with delay stabilization. OD denotes an optical diplexer.

The paper starts from defining the general frequency accuracy and stability requirements for long-distance, ultra-accurate time transfer links, and then analyses the details of the conversion of the high-frequency beat note, with the offsets extending up to 50 GHz, into the intermediate frequency (IF) range. Next, we focus on two specific sources of frequency errors that may occur in the considered circuits. They are related to the lasers' phase noise and the operation at low optical powers. The countermeasures to reduce the mentioned errors and extend the input power operation range are proposed. Finally, the experimental results concerning the stability and accuracy obtained with both relatively wide line width telecom-grade DFB lasers, and also with lower noise integrated tunable laser assemblies (ITLA) are provided.

II. Accuracy and Stability Requirements

One of the main accuracy limits of time transfer in any bi-directional link is related to determining its asymmetry. Considering, as an example, the link with the stabilized propagation delay sketched in Fig. 1, it can be shown that the relation between the input t_{L} and output t'_{L} time scales is [27]:

$$t'_L = \frac{T_{RT}}{2} + \frac{\tau_C}{2} + \frac{\Delta\tau_A}{2} + t_L, \tag{1}$$

where $T_{RT} = t''_L - t_L$ is the round-trip propagation delay, t''_L is the timescale reflected back to the local terminal, τ_C is a calibration constant, combining all instrumental asymmetries of the local and remote terminals, and $\Delta\tau_A$ is the asymmetry related to the fiber optic path. A substantial part of the asymmetry, denoted further as $\Delta\tau_{FB}$, is caused by the chromatic dispersion of the fiber due to the difference of the optical frequencies $\Delta\nu_{FB} = \nu_F - \nu_B$, used to convey signals between the local and remote terminals in the forward (ν_F) and backward (ν_B) directions. It can be calculated as:

$$\Delta\tau_{FB} = c/(\nu_F\nu_B) \cdot D \cdot L \cdot \Delta\nu_{FB}, \tag{2}$$

where D is a chromatic dispersion coefficient, L is the length of the link and c is the speed of light.

To determine $\Delta\tau_{FB}$ accurately, a known frequency shift $\Delta\nu_M$ can be applied during the link calibration [13], that results in a change of the delay $\Delta\tau_M$ measured at the link's local terminal. $\Delta\tau_{FB}$ is related to $\Delta\tau_M$ by:

$$\Delta\tau_{FB} = \Delta\tau_M \frac{\Delta\nu_{FB}}{\Delta\nu_M}. \tag{3}$$

The resulting type B uncertainty $u_B(\Delta\tau_{FB})$ can be determined directly from (3). To get an idea of the required level of accuracy we can substitute $c/(\nu_F\nu_B)\cdot D\cdot L\cdot\Delta\nu_M$ for $\Delta\tau_M$, assume $\Delta\nu_{FB}\approx\Delta\nu_M=\Delta\nu$, and take equal uncertainties of both $\Delta\nu_{FB}$ and $\Delta\nu_M$. Then, to make the contribution of the lasers' frequency accuracies negligible (i.e., $u_B(\Delta\tau_{FB})$ not greater than, say, 1 ps) in comparison with the other contributions for links up to 1000 km long (see, e.g., [13] and [27] for extensive discussion of link calibration uncertainty and the significance of particular contributions), the required level of $u_B(\Delta\nu_{FB})$ and $u_B(\Delta\nu_M)$ is less than 5 MHz. The above estimation assumes a standard single-mode fiber (G.652 accordingly to ITU-T recommendations), with D around $17\ \mathrm{ps}\cdot\mathrm{nm}^{-1}\cdot\mathrm{km}^{-1}$ and optical frequencies around 193 THz, resulting in the coefficient $c/(\nu_F\nu_B)\cdot D\cdot L$ equal to about $1.37\cdot10^{-7}$ ps/Hz.

Fluctuations of the frequencies of the lasers in both local and remote modules also influence the stability of transferred timescale as they convert directly into fluctuations of PPS pulses. An estimation of the resulting jitter (that can be regarded as type A uncertainty contribution) can be obtained using the proportionality coefficient appearing in equation (2) as the conversion mechanism is exactly the same, i.e., the chromatic dispersion of the fiber. To be negligible when compared to other contributions (resulting, e.g., from electronic components, Rayleigh backscattering and amplified spontaneous emission of the optical amplifiers [23]), the root-mean-square (RMS) value of this jitter should not exceed 1 ps. This requires the RMS fluctuations of the relative frequency of the lasers not greater than about 7 MHz for a 1000 km long link using G.652 fiber. This value is larger than 5 MHz mentioned in the paragraph just above because now only $\Delta\nu_{FB}$ contributes the result, whereas previously also $\Delta\nu_M$ had to be included.

Another measure used to express stability of timing signals is its time deviation (TDEV) plotted versus averaging time τ , which is also affected by lasers frequency fluctuations. For some particular value of τ the TDEV depends on the spectral distribution of frequency fluctuations so there is no direct connection to their RMS value. Nevertheless, contribution of the resulting jitter can be regarded as negligible if its TDEV is not greater than about 100 fs for $\tau>1\,\mathrm{s}$ [23].

The requirements concerning both accuracy and stability can be, in principle, relaxed (i.e., increased) about three times if a G.655 non-zero dispersion shifted (NZDS) fiber is available due to its reduced chromatic dispersion. This, however, is rarely the case in practice.

III. Idea of Laser Frequency Stabilization

The general idea of a frequency synchronized laser module (FSLM) considered herein is based on beating the optical fields from two lasers (the reference ν_R and stabilized ν_S ones) using a high-speed photodiode and comparing the frequency of the resulting electrical signal with a reference frequency f_{CLK} derived from a stable crystal oscillator (XO). The error signal is then used in a feedback loop, which controls ν_S to drive this error to zero (Fig. 2).

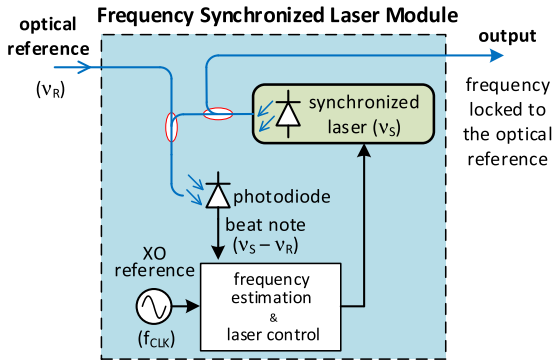

Fig. 2. A general concept of a system allowing locking the laser frequency to an optical reference.

The time transfer system, exploiting such FSLMs, can be organized in several ways, differing in the origin of the optical reference signal and the type of the synchronized laser used. In the simplest case, the optical reference signal comes from a far-end terminal of the link (e.g., if the remote end is synchronized, the synchronization is based on the local terminal laser), and is thus intensity-modulated by the timing signal containing PPS markers. The signal from the synchronized laser, which undergoes beating with the optical reference signal, can either be intensity-modulated or not, depending on whether the modulator is integrated with the synchronized laser (as is e.g., in DFB lasers with embedded electro-absorption modulators), or is external (as is when a LiNbO3 Mach-Zehnder modulator is used).

A different and much more-sophisticated time transfer system can be built jointly with an optical frequency transfer link [32]–[35]. In such a transfer system the clean and un-modulated optical carrier can be simultaneously used as a source of the reference frequency to mutually lock the lasers used to transfer time. Such a system not only offers the ultimate performance, but also allows joint transfer of all metrological signals (i.e., time, radio and optical frequencies) over the same optical fiber, packed within a small piece of optical spectrum.

In any case, the optical reference for FSLM needs to be derived from the signal used to convey the time or frequency information and this should not degrade the sensitivity of the time transfer system itself. In addition, when one or both lasers are intensity modulated with the PPS markers, the beating current is also modulated, which reduces the average signal available for the control circuitry. This means that the FSLM should be able to operate with weak input signals, in practice well below -30 dBm. Thanks to the beating of the two optical fields in a high-speed photodiode, the resulting time-varying current contains a factor proportional to the product of weak reference E_R and strong local E_S fields, resulting in an apparent gain. This photocurrent is equal to:

$$i_B(t)=2\mathcal{R}\cdot E_S\cdot E_R\cdot\cos\left(2\pi f_B t+\varphi(t)\right), \tag{4}$$

where $f_B=\nu_S-\nu_R$ is the beat frequency, $\mathcal{R}$ is the sensitivity of the photodiode, $P_R=|E_R|^2$ and $P_S=|E_S|^2$ are the optical powers of the reference and synchronized lasers, respectively, and $\varphi(t)$ is the component due to the phase noise of the involved

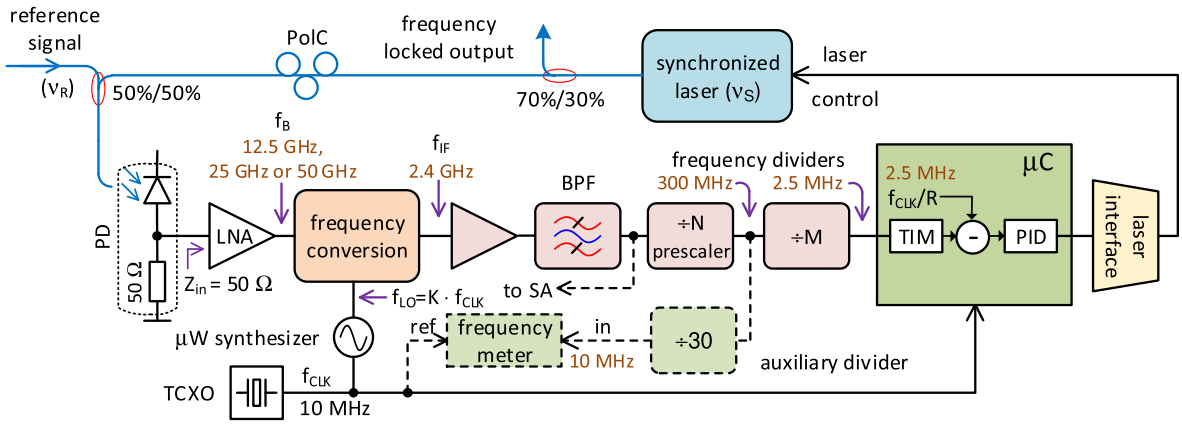

Fig. 3. Block diagram of the FSLM considered in the paper. Connections to measuring instruments are shown with the dashed lines. PD denotes a high-speed photodiode, BPF a band-pass filter, PolC a polarization controller and SA a spectrum analyser.

lasers. It should be noted that eq. (4) is valid only if the polarization alignment of the two laser fields involved is assured, so some form of polarization control is necessary. Otherwise the strength of the beat signal will be lower and may be not enough for reliable operation of the FSLM.

For the setup described here the direct measurement of the frequency of the beat note is difficult as its frequency is equal to the frequency offset between the two lasers (so it is either 12.5 GHz, 25 GHz or 50 GHz), so a suitable high-frequency prescaler must be used before applying the signal to the frequency counter.

For a reliable operation of any high-speed prescaler relatively high input power level is required, at least -15 dBm [36] (or even more for some 50 GHz devices [37]). Assuming a minimum acceptable value of the optical powers $P_R = -30\,\mathrm{dBm}$, taking $P_S \sim +3\,\mathrm{dBm}$ and $\mathcal{R} = 0.8\ \mathrm{A/W}$, the power incident the amplifier following the photodiode is about -45 dBm provided no additional signal losses occur, e.g., due to polarization misalignment. In addition, when one or both lasers are intensity modulated, the beat current is also modulated, so the signal available for the prescaler is even further reduced. The gain of at least 30 dB needs thus to be provided prior entering the prescaler. It is more convenient to implement only a first low noise amplifier (LNA) directly at the beat frequency, and to shift the rest of the necessary amplification to some lower intermediate frequency f_{IF} resulting from a frequency down-conversion.

The block diagram of discussed lasers synchronization system is presented in Fig. 3. The intermediate frequency f_{IF}, although arbitrary to some extent, was chosen in our case as equal to 2.4 GHz (the consequence of this choice will be discussed in more details in sections V and VI.B). The details of the frequency conversion block depend on the required offset between the forward and backward lasers. The most concern here was, despite its high operation frequency, this block had to be realized using commercially available components only, requiring neither sophisticated and expensive microwave bonding techniques, nor special microwave substrates. In case of 12.5 GHz offset, a simple mixer can be used as the required local oscillator frequency of $f_{LO} = 10.1\,\mathrm{GHz}$ can be easily provided by commercially available, integrated microwave synthesizers (e.g., ADF5610 from Analog Devices). For the offset equal to 25 GHz a 2nd order harmonic mixer is more suitable, allowing decreasing f_{LO} to a manageable value of 11.3 GHz. An offset equal to 50 GHz requires a two-stage frequency conversion, otherwise either a high order of harmonic mixing with high conversion loss or inconveniently high f_{LO} is necessary. Proposed structures are shown in Fig. 4. For both 12.5 GHz and 25 GHz offsets image rejection mixers were used to limit the amount of noise interfering with detected signals. To realize FSLM with 50 GHz offset we decided to use ordinary double balanced mixers due to simpler construction of the 50 GHz part of the circuit.

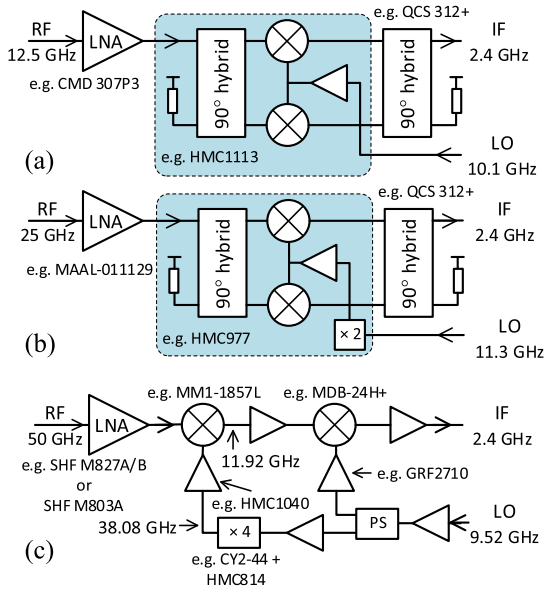

Fig. 4. Details of frequency conversion block for offsets of: 12.5 GHz (a), 25 GHz (b) and 50 GHz (c). PS denotes a power splitter. The high-speed photodiodes used to drive the conversion blocks were PD-30 (Optilab) for (a) and (b), and XPVD2120 (Finisar) for (c). The part numbers given are those used for the actual manufacturing and evaluation of modules. They do not represent a recommendation, as other models from other manufacturers may also be available.

After frequency conversion, the signal is band-pass filtered and applied to a high-speed prescaler, dividing the frequency by $N = 8$ to 300 MHz. The next stage divides the frequency by $M = 120$, reducing it to 2.5 MHz. Such a low value can be conveniently processed using a timer (TIM) embedded in a microcontroller (μC) by counting a number of cycles in a reference time interval. The μC is also responsible for running a proportional-integral-derivative (PID) regulator and providing a feedback signal to the laser via a suitable interface.

The polarization alignment was obtained by inserting a polarization controller at the output of the synchronized laser (PolC - see Fig. 3). The adjustment was done manually only once during setting up the entire circuit. However, for a reliable and human intervention free operation in a "live" time- transfer system, this adjustment should be automatized. This could be done by adjusting the polarization to maximize the strength of the IF signal in a feedback loop.

The FSLMs we tested used two types of telecom-grade lasers, namely thermally-tuned DFB ones with an integrated electro-absorption modulator, or an integrated tunable laser assemblies (ITLA), allowing digital tuning with a 1 MHz resolution via a designated ITLA multi-source agreement (MSA) serial interface. The ITLA was operated in so-called whisper mode, which is a manufacturer-specific (the ITLA used was Pure Photonics PPCL200 model) low phase noise mode, where the activity of ITLA internal control loops is limited.

IV. Fundamental FSLM Accuracy

The fundamental limit on the FSLM accuracy is related to the uncertainty $u(f_{CLK})$ of the clock oscillator feeding the microwave synthesizer and simultaneously driving the TIM clock used to count the frequency inside the μC. Considering the equilibrium condition of the feedback loop shown in Fig. 3 and taking details of the frequency conversion block (Fig. 4) into account, one can observe that:

$$f_B = (M \cdot N/R + K \cdot Q) \cdot f_{CLK}, \tag{5}$$

where the meaning and values of the coefficients M and N have already been defined, and R is the ratio between f_{CLK} and the frequency measured using the TIM (being 2.5 MHz in our case, so $R = 4$). The two remaining coefficients are related to the generation of f_{LO} by the microwave synthesizer (K) and its multiplication inside the frequency conversion block (Q). Their values depend on the offset between the lasers, and in our implementations are: $K = 1010, Q = 1$ for 12.5 GHz, $K = 1130, Q = 2$ for 25 GHz and $K = 952, Q = 5$ for 50 GHz.

It stems from (5) that f_{CLK} and f_B are proportional, so their relative accuracies must be the same. Assuming that the system is driven by a standard temperature compensated crystal oscillator (TCXO) with the accuracy of ± 2.5 ppm, the worst-case uncertainty (i.e., for 50 GHz offset) is below 80 kHz. For lower offsets, the uncertainties are proportionally smaller and are below 40 kHz and below 20 kHz for the offsets of 25 GHz and 12.5 GHz, respectively. It is so obvious that the beat-note accuracy possible with FSLM is well below the requirements formulated in Section II, even with a standard TCXO used as a f_{CLK} source. This uncertainty can be reduced by locking the TCXO to a superior source such as an H-maser, when operating the system e.g., in a T&F lab. There are, however, other sources of possible errors in the FSLM approach, which need to be considered. These are addressed below.

V. IF-Related Constraints

As it has already been mentioned, the choice of IF is to some extent arbitrary. There are, however, constraints related to the fact that the beating process is insensitive to the sign of the resulting frequency. In case the frequency of the synchronized laser is at the wrong side of the reference one (either permanently due to its too large initial offset after powering on the FSLM, or temporarily because of too large instantaneous laser noise), the sign of feedback appears to be positive instead of negative, resulting in tuning the synchronized laser in a wrong direction, and causing system malfunction. To solve this problem the IF frequency needs to be relatively high to allow for a reasonable offset or noise. It is also desirable that the bandwidth of the IF amplifier is relatively large, so that the signal frequency at the input of the prescaler does not temporarily drop to too small values, which, in turn, causes the system to malfunction. This problem is especially important because the lasers used for time transfer applications (like telecom DFB and ITLA types) show substantial amount of phase noise, characterized by a full width at half maximum ($FWHM$) line widths exceeding 10 MHz.

Apart from the system malfunction, a systematic error can occur when the IF frequency is set too low in comparison to the spectral line width of the lasers involved. As the frequency conversion does not affect the phase noise $\varphi(t)$ (see (4)), it appears directly at the IF side of the FSLM. Its rate of change $d\varphi/dt$ depends on the bandwidth of the phase noise, so it rises relatively to IF when decreasing the nominal f_{IF} value. This results in a more and more noisy character of the IF signal. If the instantaneous value of $d\varphi/dt$ divided by 2π is comparable to f_{IF}, a phase reversal can occur, giving rise to an extra zero-crossing in the resulting signal, which can be counted by the fast prescaler (the N-divider in Fig. 3). This way the estimated frequency obtained by counting signal slopes within a reference time interval is apparently increased. The resulting error (frequency shift) is further compensated by the control loop, causing a too low optical frequency ν_S of the synchronized laser.

To determine the impact of discussed effect, an open-loop measurement was set up with the BPF removed and two DFB lasers locked to individual wavelength lockers. The resulting frequency error was assessed by measuring the signal at the output of the auxiliary divider while changing the LO frequency over a broad range. In addition, the FWHM of one of the lasers was changed by adjusting its bias current. As it can be seen from Fig. 5, the error can be huge, but drops quickly to a value around 10^{-6} when the ratio $FWHM/f_{IF}$ is below a few times 10^{-2}. This calls for f_{IF} about two to three orders of magnitude higher than the lasers $FWHM$, requiring f_{IF} to be in some low-GHz range. This will assure the resulting error not greater

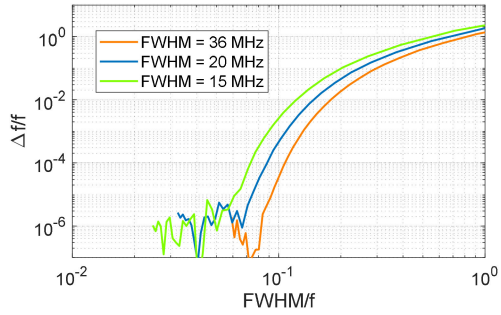

Fig. 5. Relative systematic frequency error resulting from laser phase noise.

than a fraction of MHz, making the problem negligible for any DFB laser here (cf. Section II).

VI. Experimental Results

The FSLMs built accordingly to the ideas presented in the previous sections have been tested and the frequency stability and accuracy has been assessed.

A. FSML Frequency Stability

To assess the stability of the optical frequency difference of the two lasers we used a frequency counter (PikTime T4100U) connected to the output of an auxiliary, dividing-by-30 frequency divider (see Fig. 3). Any frequency fluctuations observed there, after scaling by 30, reflects directly the fluctuations of the beat note. The measurements were performed in a non-air-conditioned laboratory with temperature fluctuations about 5 °C, and with the reference signal power set to −30 dBm. The lasers used were telecom grade DFB and ITLA types, operating near 1549.32 nm, referenced either to the same type laser or to a 1550 nm RIO Orion module.

Representative examples of the lasers differential frequency fluctuations, observed for a few days in the FSLM with an offset of 25 GHz, are shown in Fig. 6. In both cases the plots are similarly smooth, without any tendency to a drift, which suggests correct operation of the FSLM concept. Assuming a 1000 km long link using G.652 fiber, the jitter contribution resulting from the observed RMS fluctuations will be less than 240 fs, which is well below the requirements formulated in Section II. Other examined circuits, using different frequency offset (i.e., 12.5 GHz and 50 GHz), showed similar behavior.

The results of the FSLMs stability assessment are collected in Fig. 7, where the TDEV contribution due to lasers frequency fluctuations calculated for a chromatic dispersion equivalent to a 1000 km long link using a G.652 fiber is shown. The TDEV curves for all examined circuits start below 200 fs at τ equal to 0.1 s and then drop down gradually for averaging times greater than 1 s. A basic source of frequency fluctuations in FSLM can be related to the method of frequency estimation in the control loop, which is based on counting slopes (full cycles) in a reference time interval. This results in a white frequency modulation (WFM) noise due to integer-rounding. This converts into a white phase modulation (WPM) of the PPS signal edges through the chromatic dispersion of the fiber, so a slope of TDEV

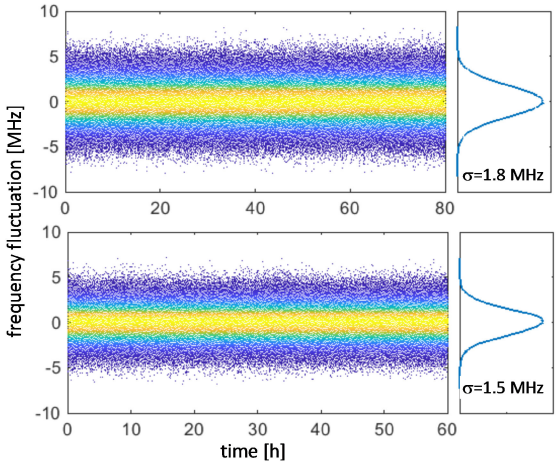

Fig. 6. Frequency fluctuation of an ITLA laser synchronized to a RIO Planex (upper) and of a DFB laser synchronized to another DFB (lower) with the frequency offset between the two lasers set to 25 GHz. Right insets show the histograms with the standard deviation. Gating time of the frequency meter was set to 100 ms.

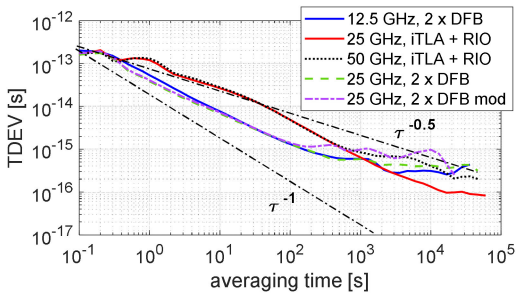

Fig. 7. Plots of TDEV calculated for dispersion equivalent to 1000 km of G.652 fiber link using FSLM with different offsets. The case when two intensity modulated DFB lasers were frequency locked to eachother is also shown.

curves close to $\tau^{-1/2}$ can be expected. Inspection of Fig. 7. shows actual slopes between τ^{-1} and $\tau^{-1/2}$, so other sources of fluctuations need evidently be present. The pedestal noticeable below 10^{-15} suggests presence of some flicker component also.

For the averaging times shorter than about 100 s the DFB lasers show slightly less noise than ITLA ones. The most probable reason of such a behavior is due to the method of laser tuning. The frequency of the DFB lasers have been changed by fine-tuning their temperature using a Peltier cooler, whereas the resolution of changing the ITLA frequency was limited by the digital MSA interface to crude 1 MHz only (in both cases the frequency was updated 100 times per second). In addition, the response of the ITLA used showed some 1 Hz ringing to the frequency change command, which is visible as a bump around $\tau = 1$ s on respective TDEV curves. Nevertheless, obtained results are more than satisfying with respect to the requirements given in Section II, especially for the averaging times exceeding 10 s. Their exact character depends to some extent on the parameters of the PID controller, which has been trimmed experimentally to obtain the best results.

The impact of the intensity modulation, used to convey the T&F signals, has also been investigated for the case of using two

DFB lasers equipped with internal electro-absorption modulators. To prevent the amplitude of the beat from decreasing too much when the modulator is in its "off" state, the power extinction of the modulated signals was set to 60%, which corresponds to about 37% in terms of the electric field strength. As it can be seen from the curve shown in Fig. 7., there is no evidence of the modulation impact noticeable, as the TDEV curves for the un-modulated and modulated cases are very similar.

B. FSLM Accuracy Under Low-Level Operation

The last point that needs investigation is the influence of the power of the reference optical signal to the FSLM behavior. In the FSLM the frequency of the beat note is estimated by counting the slopes of the divided IF signal (Fig. 3). As the power of the reference signal gets lower, the noise term entering the fast prescaler, forming the first stage of the divider chain, becomes more and more important. Because of the low resistive load $R_L = 50\,\Omega$ of the high-speed photodiode, the contribution of its thermal noise is comparable to the contribution of the shot noise of the synchronized laser (their spectral densities are kT and $q\mathcal{R}P_S R_L/2$, respectively, where k is the Boltzmann constant and q is the electron charge). As a result, the equivalent noise power density referenced to the LNA input (including both shot and thermal components and assuming LNA noise figure of 2.5 dB) can be estimated at the level of -168.6 dBm/Hz for optical powers $P_S = +3$ dBm and $P_R = -30$ dBm. Assuming total IF gain and bandwidth used in the manufactured prototypes of about 60 dB and 1 GHz, respectively, the noise at the input of the prescaler can be estimated as about -18.6 dBm, so it is relatively large.

As the power of the optical reference signal becomes lower, the band-pass noise mentioned above starts to influence the prescaler more and more, and becomes a source of frequency errors when the frequency is estimated by counting the number of cycles within the reference time interval. It should be emphasized that this phenomenon, which requires the presence of relatively strong noise at the input of the prescaler, differs substantially from a well-known self-oscillation of prescalers that occurs at low input powers [36], [38]. As up to authors' knowledge there is no good theory explaining the observed effect and allowing predicting occurring frequency error [39], [40], we decided to perform a set of experiments, where the photodiode (see Fig. 3) has been exchanged with a variable-power microwave generator. The measurement results shown in Fig. 8 were for three different prescaler models configured to divide-by-eight and rated for 4 GHz, 6.5 GHz and 12 GHz operation (HMC988, HMC705 and HMC363, respectively, all from Analog Devices). The frequency of the signal applied to the LNA was set to either 25.72 GHz or 24.76 GHz (corresponding to f_{IF} under high SNR equal to 3.12 GHz or 2.16 GHz, respectively). The mid-frequency of a band-pass noise entering the prescalers was $f_0 \approx 2.5$ GHz (because of BFCN-2500+ filter from Mini-Circuits used to shape the spectrum). As it can be seen in the inset, the error changes its sign, depending on the position of the signal frequency with respect to the noise center frequency f_0. The value of the error can reach large values, but

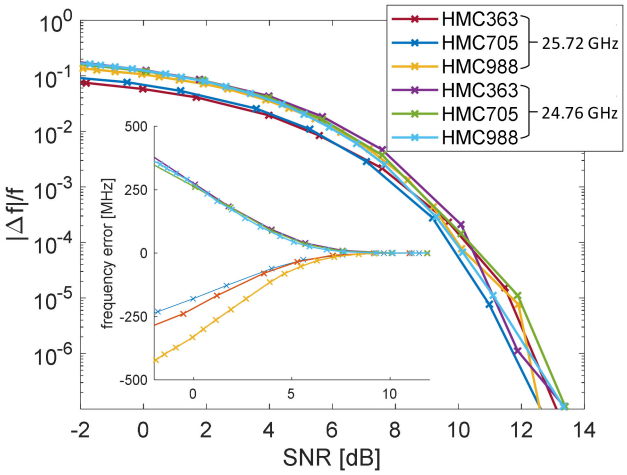

Fig. 8. Frequency error caused by noise present at the input of a high-speed prescaler. The inset shows absolute frequency errors including their sign.

decreases, as it might be expected, when increasing the SNR at the prescaler input. For SNR around 12 dB the relative error drops to about 10^{-6} (i.e., an absolute frequency error is below a few MHz), so may be regarded as negligible in the considered application (cf. Section II). It is also visible that all examined prescalers share rather similar overall behavior.

It is worth to note that the slope-counting system still shows some relatively well-defined number of counts in a reference time interval, even without any periodic component at its input, when substantial amount of noise is present (as is in our case). Theoretical analysis of such a case, when only a band-pass noise centered around f_0 contained in a range $f_0 \pm f_C$ is applied to the input of a threshold detector [39], leads to a "mean" frequency f_N equal to:

$$f_N = \sqrt{f_0^2 + f_C^2/3}, \tag{6}$$

which is located slightly above the filters center frequency (it can be estimated to be about 2517 MHz basing on the BFP datasheet). This property is interesting in that the noise can be seen as a means of preventing the self-oscillation of the prescaler that occurs when a noise-free but weak periodic signal is applied to its input. If the power of the signal is increased, the output frequency can be expected to change gradually rather than the self-oscillation abruptly dying out after a certain signal level is exceeded. On the other hand, the presence of the noise is penalized with the systematic error mentioned above. But, as discussed in Section II, this can be accepted to some extent in FSLM.

To check the behavior of the complete FSLM system to low optical reference power levels, we investigated the actual value of the IF frequency directly at the output of the amplifier driving the prescaler. In a closed-loop system the f_{IF} will deviate from its nominal value because of the negative feedback, tending to keep the frequency at the output of the divider chain (see Fig. 3) at 2.5 MHz. Any deviation observed there is thus one-to-one related to the actual value of the offset frequency between the synchronized and the reference lasers. To avoid potential frequency error when measuring the frequency at low signal

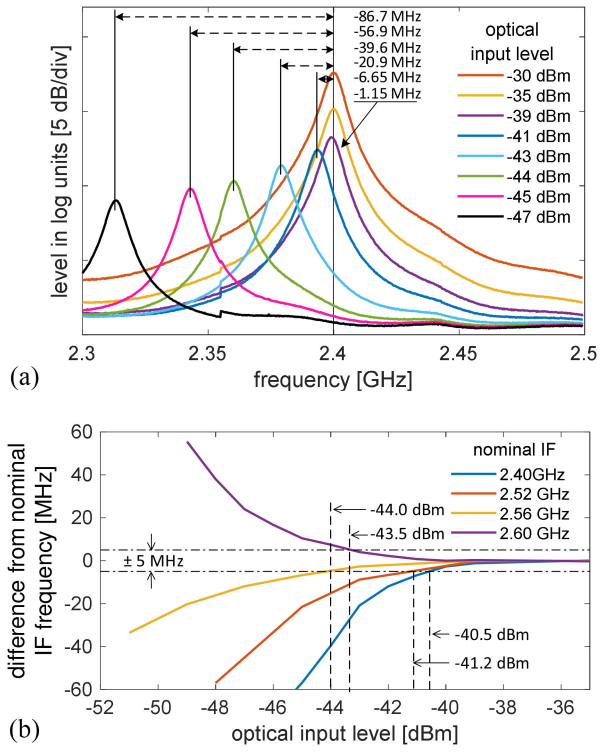

Fig. 9. Spectra measured at the prescaler input for various reference optical power levels for the 25 GHz offset FSLM using DFB laser (a) and a deviation from the nominal f_{IF} for a few nominal IF values (b).

levels, we used a spectrum analyzer to record the spectra at the prescaler input instead of a frequency meter. The frequency was then estimated as a value corresponding to the maximum of the spectrum curve. The measurements were performed in the FSLM with 25 GHz offset using a DFB laser and HMC988 prescaler.

The results collected in Fig. 9(a), show clearly a systematic negative shift of the peak frequency of the respective curve with respect to the nominal value of 2.4 GHz occurring when the input power decreases. For optical reference signal levels larger than -35 dBm no evidence of any error is observed. Taking into account the acceptable frequency error requirements discussed in Section II, the minimum optical reference signal power level required by FSLM can be estimated as about -40 dBm. At even lower power levels the resulting error can, in principle, be eliminated, by a corresponding frequency shift in the microwave synthesizer if it is made dependent on the level of the signal reaching the prescaler. However, such an approach is not recommended as it complicates circuit design and requires additional initial calibration steps.

Noting that the noise-induced frequency error may be expected to depend on the relation between the nominal f_{IF} value and f_N, another and particularly simple solution can be proposed, by trying to make these two frequencies coincide. This, however, requires a trial-and-error approach, as the accurate value of f_N depends on the actual shape of the BPF frequency characteristic and the prediction given by (6) is rather crude. The effects are shown in Fig. 9(b), where it is visible that setting f_{IF} around 2.56 GHz (instead of our initial choice of $f_{IF} =$ 2.4 GHz, giving $f_N - f_{IF} \approx 117$ MHz as estimated from eq. (6)) can indeed lower the range of stable FSLM operation to about -44 dBm, and remaining within the permissible frequency error margins.

VII. Conclusion

Ultra-accurate fiber optic time transfer requires high accuracy and stability of the frequencies of the lasers used to convey timing information. This is necessary to mitigate the contribution of the fiber chromatic dispersion to the calibration uncertainty. The technique investigated in this paper and using relative locking of the frequencies of lasers is suitable to keep this contribution below 1 ps for links up to 1000 km, which makes it negligible with respect to other contributions (related e.g., to time interval measurements [41] or the Sagnac effect [42]). The contribution to the time transfer instability has been estimated as not greater than 100 fs when expressed as TDEV for the averaging times greater than 1 s, and below 240 fs if the RMS jitter is considered. Proposed circuits can be built from commercially available electronic components and do not require temperature-controlled conditions or calibration.

Using the proposed technique the lasers in the end terminals of the basic bi-directional setup of a time transfer link can be mutually frequency locked (e.g., the remote terminal one to the local one) or, if a stable optical frequency is also involved (e.g., in a hybrid transfer system which delivers time, electrical and optical frequencies simultaneously), it can serve as an auxiliary optical reference for the lasers at both ends of the link.

The problem of the reference optical power level required by the FSLM to operate reliably has been investigated and it was found that the limit results from band-pass noise, which is responsible for systematic frequency error, occurring in the high-speed prescaler when the SNR at its input is below about 12 dB. The particular error value depends not only on the SNR, but also on the difference between the nominal f_{IF} value, the noise center frequency and the noise bandwidth. The circuits that have been evaluated allow operation down to about -40 dBm of the optical reference signal without introducing systematic frequency error exceeding 5 MHz. By fine-tuning the nominal f_{IF} value it was possible to push the FSLM sensitivity down to -44 dBm, gaining about 4 dB.

So the interesting question arises, how far the sensitivity limit can be pushed by the clever placement of the intermediate frequency. Looking at Fig. 9(b) it seems that a value of f_{IF} exists that makes the error curve flat. However, for low enough power levels the feedback loop in the system will become effectively broken, making the laser tuning signal depending only on noise, so the frequency locking must finally fail. This problem has not been analyzed thoroughly and requires further investigation.

A solution capable of eliminating the frequency error completely is using a tracking filter based on a phase locked loop (PLL), placed at the front of the prescaler. Weighing complexity against ease of implementation, we have not used this option so far.

Another problem that needs to be discussed concerns the consequences of reducing the extinction (mentioned at the end of

section VI.A), which is required for the operation of the FSLM in an intensity-modulated based system. This reduction leads to a so-called extinction penalty, which effectively decreases the sensitivity of the time transfer system. Assuming the extinction reduction from 85% to 60% (as in our experiments), the penalty is only about 1.5 dB, which can easily be compensated by increasing the gains of the optical amplifiers installed along the fiber link. In addition, there is still room for optimization here, as a further reduction of the minimum power required by the FSLM still seems possible.

REFERENCES

[1] L. Essen and J. V. L. Parry, "The caesium resonator as a standard of frequency and time," *Philos. Trans. Roy. Soc. A*, vol. 250, pp. 45–69, 1957.

[2] S. Weyers *et al.*, "Advances in the accuracy, stability, and reliability of the PTB primary fountain clocks," *Metrologia*, vol. 55, pp. 789–805, 2018, doi: 10.1088/1681-7575/aae008.

[3] J. Guéna *et al.*, "First international comparison of fountain primary frequency standards via a long distance optical fiber link," *Metrologia*, vol. 54, pp. 348–354, 2017, doi: 10.1088/1681-7575/aa65fe.

[4] A. Ludlow *et al.*, "Optical atomic clocks," *Rev. Modern Phys.*, vol. 87, pp. 637–701, 2015, doi: 10.1103/RevModPhys.87.637.

[5] W. F. McGrew *et al.*, "Towards the optical second: Verifying optical clocks at the SI limit," *Optica*, vol. 6, no. 4, 2019, doi: 10.1364/OPTICA.6.000448.

[6] P. Delva *et al.*, "Test of special relativity using a fiber network of optical clocks," *Phys. Rev. Lett.*, vol. 118, 2017, Art. no. 221102, doi: 10.1103/PhysRevLett.118.221102.

[7] P. Morzyński *et al.*, "Absolute measurement of the $^{1}S_0$-$^{3}P_0$ clock transition in neutral ^{88}Sr over the 330 km-long stabilized fibre optic link," *Sci. Rep.*, vol. 5, pp. 17495–17499, 2015, doi: 10.1038/srep17495.

[8] B. Wang *et al.*, "Square kilometre array telescope—Precision reference frequency synchronisation via 1f-2f dissemination," *Sci. Rep.*, vol. 5, 2015, Art. no. 13851, doi: 10.1038/srep13851.

[9] C. Clivati *et al.*, "A VLBI experiment using a remote atomic clock via a coherent fibre link," *Sci. Rep.*, vol. 7, 2017, Art. no. 40992, doi: 10.1038/srep40992.

[10] P. Krehlik *et al.*, "Fibre-optic delivery of time and frequency to VLBI station," *Astron. Astrophys.*, vol. 603, 2017, Art. no. A48, doi: 10.1051/0004-6361/201730615.

[11] T. Mehlstaubler *et al.*, "Atomic clocks for geodesy," *Rep. Prog. Phys.*, vol. 81, 2018, Art. no. 064401, doi: 10.1088/1361-6633/aab409.

[12] P. Tavela and G. Petit, "Precise time scales and navigation systems: Mutual benefits of timekeeping and positioning," *Satell. Navig.*, vol. 1, no. 10, 2020, doi: 10.1186/s43020-020-00012-0.

[13] Ł. Śliwczyński *et al.*, "Calibrated optical time transfer of UTC(k) for supervision of telecom networks," *Metrologia*, vol. 56, 2019, Art. no. 015006, doi: 10.1088/1681-7575/AAEF57.

[14] Ł. Śliwczyński *et al.*, "Fiber-based UTC dissemination supporting 5G telecommunications networks," *IEEE Commun. Mag.*, vol. 58, no. 4, pp. 67–73, Apr. 2020, doi: 10.1109/MCOM.001.1900599.

[15] A. Derviskadic, R. Razzaghi, Q. Walger, and M. Paolone, "The white rabbit time synchronization protocol for synchrophasor networks," *IEEE Trans. Smart Grid*, vol. 11, no. 1, pp. 726–738, Jan. 2020, doi: 10.1109/TSG.2019.2931655.

[16] J. Lopez-Jimenez, J. Luis Gutierrez-Rivas, E. Marin-Lopez, M. Rodriguez-Alvarez, and J. Diaz, "Time as a service based on white rabbit for finance applications," *IEEE Comm. Mag.*, vol. 58, no. 4, pp. 60–66, Apr. 2020, doi: 10.1109/MCOM.001.1900602.

[17] D. Valat and J. Delporte, "Absolute calibration of timing receiver chains at the nanosecond uncertainty level for GNSS time scales monitoring," *Metrologia*, vol. 57, 2020, Art. no. 025019, doi: 10.1088/1681-7575/ab57f5.

[18] Z. Jiang *et al.*, "Improving two-way satellite time and frequency transfer with redundant links for UTC generation," *Metrologia*, vol. 56, 2019, Art. no. 025005, doi: 10.1088/1681-7575/aafced.

[19] M. Lombardi, "An evaluation of dependencies of critical infrastructure timing systems on the global positioning systems (GPS)," NIST Techn. Note 2189, NIST, 2021, doi: 10.6028/NIST.TN.2189.

[20] M. Rost *et al.*, "Time transfer through optical fibers over a distance of 73 km with an uncertainty below 100 ps," *Metrologia*, vol. 49, pp. 772–778, 2012, doi: 10.1088/0026-1394/49/6/772.

[21] G. Wu, L. Hu, H. Zhang, and J. Chen, "High-precision two-way optic-fiber time transfer using an improved time code," *Rev. Sci. Instrum.*, vol. 85, 2014, Art. no. 114701, doi: 10.1063/1.4900578.

[22] J. Kodet *et al.*, "Two-way time transfer via optical fiber providing subpicosecond precision and high temperature stability," *Metrologia*, vol. 53 no. 18, 2016, doi: 10.1088/0026-1394/53/1/18.

[23] P. Krehlik, Ł. Śliwczyński, Ł. Buczek, J. Kołodziej, and M. Lipiński, "ELSTAB-Fiber optic time and frequency distribution technology - A general characterization and fundamental limits," *IEEE Trans. Ultrason. Ferroelect. Freq. Control*, vol. 63, no. 7, pp. 993–1004, Jul. 2016, doi: 10.1109/TUFFC.2015.2502547.

[24] W. Chen *et al.*, "Joint time and frequency dissemination network over delay-stabilized fiber optic links," *IEEE Photon. J.*, vol. 7, no. 3, Jun. 2015, Art. no. 7901690, doi: 10.1109/JPHOT.2015.2426874.

[25] F. Zuo *et al.*, "WDM-based fiber optic time synchronization without requiring link calibration," *IEEE Access*, vol. 8, pp. 114656–114661, 2020, doi: 10.1109/ACCESS.2020.3003702.

[26] F. Zuo, K. Xie, L. Hu, J. Chen, and G. Wu, "13 134-km fiber-optic time synchronization," *J. Lightw. Technol.*, vol. 39, no. 20, pp. 6373–6380, Oct. 2021, doi: 10.1109/JLT.2021.3102674.

[27] Ł. Śliwczyński, P. Krehlik, Ł. Buczek, and H. Schnatz, "Picoseconds-accurate fiber-optic time transfer with relative stabilization of lasers wavelengths," *J. Lightw. Technol.*, vol. 38, no. 18, pp. 5056–5063, Sep. 2020, doi: 10.1109/JLT.2020.2999158.

[28] P. Krehlik, Ł. Śliwczyński, Ł. Buczek, and J. Kołodziej, "Fiber-optic UTC(k) timescale distribution with automated link delay cancelation," *IEEE Trans. Ultrason. Ferroelect. Freq. Control*, vol. 66, no. 1, pp. 163–169, Jan. 2019, doi: 10.1109/TUFFC.2018.2878319.

[29] Athermal Fabry-Perot Wavelength Locker, Optoplex Corporation. [Online]. Available: https://www.optoplex.com

[30] T. Ikegami, S. Sudo, and Y. Sakai, *Frequency Stabilization of Semiconductor Laser Diodes*. Norwood, MA, USA: Artech House, 1995.

[31] Q. Li, L. Hu, J. Chen, and G. Wu, "Studying the double Rayleigh backscatter noise effect on fiber-optic radio frequency transfer," *IEEE Photon. J.*, vol. 13, no. 2, Apr. 2021, Art. no. 7100210, doi: 10.1109/JPHOT.2021.3058171.

[32] S. Raupach and G. Grosche, "Chirped frequency transfer: A tool for synchronization and time transfer," *IEEE Trans. Ultrason., Ferroelect., Freq. Control*, vol. 61, no. 6, pp. 920–929, Jun. 2014, doi: 10.1109/TUFFC.2014.2988.

[33] O. Lopez *et al.*, "Simultaneous remote transfer of accurate timing and optical frequency over a public fiber network," *Appl. Phys. B*, vol. 110, no. 1, pp. 3–6, 2013, doi: 10.1109/EFTF-IFC.2013.6702214.

[34] P. Krehlik, H. Schnatz, and Ł. Śliwczyński, "A hybrid solution for simultaneous transfer of ultrastable optical frequency, RF frequency and UTC time-tags over optical fiber," *IEEE Trans. Ultrason. Ferroelect., Freq. Control*, vol. 64, no. 12, pp. 1884–1890, Dec. 2017, doi: 10.1109/TUFFC.2017.2759001.

[35] X. Tian, L. Hu, G. Wu, and J. Chen, "Hybrid fiber-optic radio frequency and optical frequency dissemination with a single optical actuator and dual-optical phase stabilization," *J. Lightw. Technol.*, vol. 38, no. 16, pp. 4270–4278, Aug. 2020, doi: 10.1109/JLT.2020.2989328.

[36] D. Kim, C. Cho, J. Kim, J.-O. Plouchart, and D. Lim, "A low-power mmWave CML prescaler in 65nm SOI CMOS technology," in *Proc. IEEE Compound Semicond. Integr. Circuits Symp.*, 2008, pp. 1–4, doi: 10.1109/CSICS.2008.50.

[37] ASNT8132 DC-54GHz Broadband Clock Divider by 2, Adsantec, 2020. [Online]. Available: https://www.analog.com

[38] Frequency divider operation and compensation with no input signal, AN-1463, Analog Devices, 2017, [Online]. Available: https://www.analog.com

[39] A. Papoulis, *Probability, Random Variables Stochastic Processes*. New York, NY, USA: McGraw-Hil, 1984, pp. 345–353.

[40] W. Davenport and W. Root, *An Introduction to the Theory of Random Signals and Noise*. New York, NY, USA: IEEE Press, 1987, pp. 165–167.

[41] R. Szplet, R. Szymanowski, and D. Sondej, "Measurement uncertainty of precise interpolating time counters," *IEEE Trans. Instr. Meas.*, vol. 68, no. 11, pp. 4348–4356, Nov. 2019, doi: 10.1109/TIM.2018.2886940.

[42] J. Gersl, P. Delva, and P. Wolf, "Relativistic corrections for time and frequency transfer in optical fibers," *Metrologia*, vol. 52, pp. 552–564, 2015, doi: 10.1109/EFTF.2014.7331477.